



Advanced Gastric Cancer: CT Radiomics Prediction of Lymph Nodes Metastasis After Neoadjuvant Chemotherapy

Jia Sun¹ · Zhilong Wang² · Haitao Zhu² · Qi Yang¹ · Yingshi Sun²

Received: 7 March 2024 / Revised: 16 May 2024 / Accepted: 20 May 2024
© The Author(s) under exclusive licence to Society for Imaging Informatics in Medicine 2024

Abstract

This study aims to create and assess machine learning models for predicting lymph node metastases following neoadjuvant treatment in advanced gastric cancer (AGC) using baseline and restaging computed tomography (CT). We evaluated CT images and pathological data from 158 patients with resected stomach cancer from two institutions in this retrospective analysis. Patients were eligible for inclusion if they had histologically proven gastric cancer. They had received neoadjuvant chemotherapy, with at least 15 lymph nodes removed. All patients received baseline and preoperative abdominal CT and had complete clinicopathological reports. They were divided into two cohorts: (a) the primary cohort ($n = 125$) for model creation and (b) the testing cohort ($n = 33$) for evaluating models' capacity to predict the existence of lymph node metastases. The diagnostic ability of the radiomics-model for lymph node metastasis was compared to traditional CT morphological diagnosis by radiologist. The radiomics model based on the baseline and preoperative CT images produced encouraging results in the training group (AUC 0.846) and testing cohort (AUC 0.843). In the training cohort, the sensitivity and specificity were 81.3% and 77.8%, respectively, whereas in the testing cohort, they were 84% and 75%. The diagnostic sensitivity and specificity of the radiologist were 70% and 42.2% (using baseline CT) and 46.3% and 62.2% (using preoperative CT). In particular, the specificity of radiomics model was higher than that of conventional CT in diagnosing N0 cases (no lymph node metastasis). The CT-based radiomics model could assess lymph node metastasis more accurately than traditional CT imaging in AGC patients following neoadjuvant chemotherapy.

Keywords Gastric cancer · Lymphadenopathy · Neoadjuvant chemotherapy · Machine learning

Background

Gastric cancer is the one of the leading cause of cancer-related deaths in the world [1–3]. Locally advanced gastric cancers (LAGC) are with high risk of lymph node (LN)

metastasis and poor prognosis. The National Comprehensive Cancer Network (NCCN) proposes neoadjuvant chemotherapy (NAC) to induce tumor regression and downstaging before the surgery [4, 5]. Lymph node metastasis is a significant predictor of survival in gastric cancer [6]. Although the N stages will be done on histopathology by the nodal dissection of the radical gastrectomy after NAC, more accurate predicting nodal involvement on imaging may help surgeons detect suspicious lymph node metastases that are beyond the scope of the routine D2 lymph node dissection. Computed tomography features have the potential to predict pathological complete response (ypT0N0) after NAC in patients with LAGC [7]. Patients who had a full pathological response (pT0N0 stage) following NAC had a considerably higher chance of survival [8].

CT is an approach for preoperative staging and response evaluation of gastric cancer (GC) [7, 9–11]. CT has been a standard practice for preoperative N staging, where the identification of larger and round-shaped lymph nodes serves as an indicator of metastasis. Previous imaging

Jia Sun, Zhilong Wang, and Haitao Zhu contributed equally to this work.

Qi Yang is the lead contact.

✉ Qi Yang
yangyangqiqi@gmail.com

✉ Yingshi Sun
sys27@163.com

¹ Department of Radiology, Beijing Chao-Yang Hospital, Capital Medical University, No. 8 GongtiSouth Road, Chaoyang District, Beijing, Beijing 100020, China

² Key Laboratory of Carcinogenesis and Translational Research (Ministry of Education), Department of Radiology, Peking University Cancer Hospital & Institute, Beijing 100142, China

research studies have found that regional lymph nodes with an increased short-axis diameter greater than 10 millimeters, necrosis, or numerous clusters on imaging are suspicious for metastasis [6, 9, 12, 13]. Nevertheless, the diagnostic accuracy of computed tomography (CT) for detecting lymph node metastasis (LNM) ranges from 50 to 70% on baseline diagnosis [14–18]. FDG-PET has significantly lower sensitivity compared with CT in the detection of local lymph node involvement (56% vs. 78%), although FDG-PET has improved specificity (92% vs. 62%) [19]. Furthermore, the accuracy of restaging by computed tomography (CT) following neoadjuvant chemotherapy (NAC) remains limited in patients diagnosed with LAGC. After chemotherapy, the accuracy of CT was found to be only 37% for N staging [20]. Radiomics is a new method for quantitatively diagnosing cancer by first converting medical images into radiomics features and then choosing key aspects as the signature [21]. In recent years, there has been an increasing utilization of CT-based radiomics in the realm of stage prediction and therapy selection for patients diagnosed with advanced gastric cancer (AGC) [22–25].

Thus, present study aimed to create a radiomics model for predicting the N0 or N+ stages in LAGC following NAC.

Methods

Patients

This retrospective study was authorized and approved Ethics Committee of our hospital, and informed consent was waived due to retrospective nature. Patients were included based on the following inclusion criteria: (a) patients with histologically and CT-confirmed LAGC (cT2–4aNxM0); (b) patients who underwent radical gastrectomy and D2 lymph node dissection following two to four cycles of NAC; and (c) CT performed at baseline and less than two weeks prior to surgery. Patients were excluded based on the following criteria: (i) previous abdominal malignancies or inflammatory diseases; (ii) difficulty of tumor segmenting due to inadequate gastric distention; (iii) the adipose surrounding the stomach was almost entirely eradicated by the gastric cancer; and (iv) baseline or pre-operative CT examinations were performed at other hospitals.

We retrospectively reviewed data for 158 patients with gastric cancer who underwent surgery in two hospitals. The training cohort (125 patients) was included from Peking university cancer hospital. The testing cohort (33 patients) was included from our hospital. These patients in the training cohort were consecutively treated from January 1, 2019, to December 31, 2022. The NAC regimens for patients in training cohort included SOX (75 cases, S-1 plus oxaliplatin), XELOX (26 cases, oxaliplatin plus capecitabine), and

mFOLFOX7 (24 cases, modified regimen of leucovorin, fluorouracil, and oxaliplatin). Patients in testing cohort were consecutively treated from August 1, 2018, to December 31, 2021. The NAC regimens for patients in testing cohort included SOX (23 cases, S-1 plus oxaliplatin) and XELOX (10 cases, oxaliplatin plus capecitabine). The patients and tumor features have been summarized in Table 1. Figure 1 displays a flowchart outlining the study design employed for the creation and testing of the radiomics model.

CT Protocol

CT examinations was performed using the 64–detector row CT scanner (LightSpeed 64; GE Healthcare, Milwaukee, Wis). Each patient had been fasting for more than 8 h prior to the CT examination. To enable gastric distention and reduce gastric motility, the patients received 8 g gas-producing crystals orally before the examination. Upper abdominal unenhanced CT scans from the diaphragmatic domes to 2 cm below the lower margin of the air-distended gastric body were acquired with a collimation of 0.625 mm, 120–140 kVp, and 300–350 mAs. Subsequently, a total of 100 ml of non-ionic contrast medium (Ultravist; Schering, Berlin, Germany) was administered intravenously through an 18-gauge angiographic catheter inserted into an antecubital vein at 3 mL/sec by using an automatic injector. Contrast-enhanced CT scans were performed in the arterial phase (30 s) and in the portal venous phase (70 s). The portal venous phase was used to evaluate lymph node status. The portal venous phase axial CT images were reconstructed with a 5-mm section thickness and a 5-mm reconstruction interval for clinical interpretation and with a 0.625-mm section thickness for MPR reconstruction.

Tumor Region Segmentation

The regions of interest (ROIs) of tumor and two largest short-axis size lymph nodes were manually delineated on arterial and portal venous phase CT images by the radiologist (J.S and Z.L.W., with 10 and 12 years of experience in abdominal CT, respectively) in each center. For each CT phase, only one slice with the largest tumor area was chosen visually by the radiologist using ITK-SNAP software (version 3.6.0; <http://www.itksnap.org>). Due to the diversity and irregularity of gastric cancer morphology, it is time-consuming to manually draw the ROI of gastric cancer at all slices. Regarding lymph nodes in RECIST criteria, a maximum of two lesions from each organ are selected as representatives [26]. If too many lymph nodes are selected, some small lymph nodes may disappear after chemotherapy, making it impossible to draw the ROIs. Thus, the ROI of slices with the largest and second largest lymph node areas were manually delineated on portal venous phase CT images.

Table 1 The clinicopathological features of patients included in this study

	Training cohort (n = 125)	Testing cohort (n = 33)	P value
Sex			0.714
Female	23 (18.40%)	7 (21.21%)	
Male	102 (81.60%)	26 (78.79%)	
Age (median, range, years)	58 (27–80)	60 (46–85)	
Tumor diameter (cm)			0.704
< 4	75 (60.00%)	21 (63.64%)	
≥ 4	50 (40.00%)	12 (36.36%)	
Tumor location			0.948
Cardia	48 (38.40%)	12 (36.36%)	
Body	35 (28.00%)	10 (30.30%)	
Antrum	34 (27.20%)	10 (30.30%)	
Whole stomach	6 (4.80%)	1 (3.03%)	
Differentiation status			0.692
Well	30 (24.00%)	10 (30.30%)	
Moderate	53 (42.40%)	14 (42.42%)	
Poor and undifferentiated	42 (33.60%)	9 (27.20%)	
Lauren type			0.936
Intestinal type	54 (43.20%)	14 (42.42%)	
Diffuse or mixed type	71 (56.80%)	19 (57.58%)	
Carcinoembryonic antigen			0.198
Normal	65 (52.00%)	20 (60.61%)	
Elevated	60 (48.00%)	13 (39.39%)	
Tumor depth of invasion			0.454
ypT0-1	12 (9.6%)	4 (12.12%)	
ypT2	17 (13.6%)	8 (24.24%)	
ypT3	25 (20.00%)	8 (24.24%)	
ypT4a	66 (52.80%)	12 (36.36%)	
ypT4b	5 (4.00%)	1 (3.03%)	
Lymph node status			0.629
ypN0	45 (36.00%)	8 (24.24%)	
ypN1	21 (16.80%)	9 (27.28%)	
ypN2	27 (21.60%)	7 (21.21%)	
ypN3a	15 (12.00%)	4 (12.12%)	
ypN3b	17 (13.60%)	5 (15.15%)	

Radiomic Feature Extraction

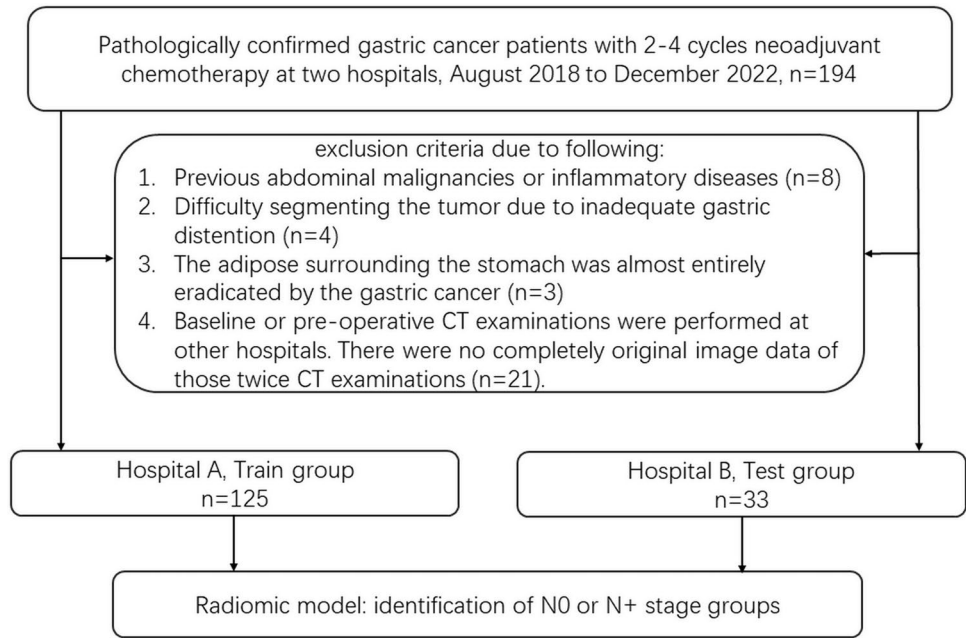
For each patient, the ROIs of tumor and lymph nodes were delineated in pretreatment and post-treatment CT images respectively, including tumor region in the artery phase, tumor region and 2 typical LNs in the venous phase. A total of 488 features were extracted from each ROI by PyRadiomics (Version 2.1.2). Totally, $488 \times 8 = 3904$ features were extracted.

Radiomic Feature Selection

Feature selection was performed according to the following steps:

1. Features from 2 LNs were averaged. A total of 488 pre-treatment LN features and 488 post-treatment LN features remained. Totally 2928 features were preserved for next step.
2. In the training group, T-test was used to remove the features that show insignificant difference ($P > 0.05$) between ypN0 and ypN+ groups. After this step, 918 features were preserved for next step. *T* value for each feature was saved for next step.
3. Correlations were calculated between each two features to avoid redundancy. If the absolute value of the Pearson correlation coefficients was larger than 0.5, the feature with the smaller *T* value was removed. After this step, 34 features were preserved for next step.

Fig. 1 Flowchart of patient selection



4. Logistic regression with least absolute shrinkage and selection operator (LASSO) was performed in the training group for both feature reduction and classification. Five-fold cross-validation was used to determine the hyperparameter that determines feature number. Finally, logistic regression returns a radiomics score by linearly combining the selected 13 features.

CT Image Analysis

The CT image analysis was performed by two radiologists with more than 10 years of abdominal diagnostic experience in the two hospitals using the workstation (Carestream Health, Shanghai, China). They reviewed the baseline and post-NAC CT images. Regional lymph nodes of gastric cancer were considered as metastases if they were solitary or separate nodes 8 mm or greater in short-axis diameter with marked enhancement, which was defined as attenuation greater than 85 HU in the post-contrast portal venous phase. Lymph nodes were also considered to represent metastases if they were cluster nodes or solitary nodes with associated reticular strands or necrosis [12].

Statistical Analysis

All the data collected in this study were analyzed using SPSS 22.0 software. Normally distributed measurement data were expressed as mean \pm standard deviation (SD), while non-normally distributed measurement data were expressed as median (interquartile range), and the comparisons were examined by Student *t*-test and Mann-Whitney

test (non-parametric distribution). The categorical data were expressed as *n* (%), and the differences between the two groups were examined by chi-square analysis or Fisher's exact test. *P* < 0.05 was considered statistically significant.

Results

After the radiomics feature selection process, 13 features (wavelet-HH_glcM_MaximumProbability, wavelet-HH_glszm_SmallAreaEmphasis, wavelet-HL_glszm_GrayLevelVariance, wavelet-LH_firstorder_Kurtosis, wavelet-HH_glszm_SmallAreaHighGrayLevelEmphasis, wavelet-HL_firstorder_Skewness, wavelet-LH_firstorder_Kurtosis, original_glszm_Zone%, wavelet-HL_gldm_DependenceVariance, wavelet-LL_firstorder_Kurtosis, wavelet-HL_glszm_LowGrayLevelZoneEmphasis, wavelet-LH_gldm_DependenceVariance, and wavelet-LH_glszm_Zone%) were selected by the linear combination with the radiomics score (Table 2).

The radiomics model based on pre- and post-neoadjuvant chemotherapy produced good results in both the training and testing cohorts (AUC 0.846 and 0.843, respectively) (Fig. 2). The sensitivity, specificity, positive predictive value, and negative predictive value in the training cohort were 81.3%, 77.8%, 86.7%, and 70.0%, respectively, and 84.0%, 75.0%, 91.3%, and 60.0% in the testing cohort (Table 3).

The results of the radiologists to diagnose a patient with or without lymph node metastasis by traditional CT

Table 2 The name, ROI, and the weight of the selected 13 features, whose linear combination contributes the radiomics score

Feature name	ROI	Weight
wavelet-HH_glcm_MaximumProbability	Tumor, pretreatment venous phase	- 0.10520695
wavelet-HH_glszm_SmallAreaEmphasis	Tumor, pretreatment venous phase	0.09908494
wavelet-HL_glszm_GrayLevelVariance	Tumor, pretreatment venous phase	0.11773877
wavelet-LH_firstorder_Kurtosis	Tumor, pretreatment venous phase	0.14998825
Wavelet-HH_glszm_SmallAreaHighGrayLevelEmphasis	LN, pretreatment venous phase	0.13529471
wavelet-HL_firstorder_Skewness	Tumor, posttreatment artery phase	- 0.08073624
wavelet-LH_firstorder_Kurtosis	Tumor, posttreatment artery phase	0.00551128
original_glszm_Zone%	Tumor, posttreatment venous phase	- 0.50605964
wavelet-HL_gldm_DependenceVariance	Tumor, posttreatment venous phase	- 0.01656421
wavelet-LL_firstorder_Kurtosis	Tumor, posttreatment venous phase	0.08016391
wavelet-HL_glszm_LowGrayLevelZoneEmphasis	LN, posttreatment venous phase	- 0.3322194
wavelet-LH_gldm_DependenceVariance	LN, posttreatment venous phase	-0.19562297
wavelet-LH_glszm_Zone%	LN, posttreatment venous phase	- 0.09276883

morphological findings were counted. The AUC, sensitivity, specificity, positive predictive value, and negative predictive value of baseline CT imaging were 0.561, 70.0%, 42.2%, 68.3%, and 44.2% in the training cohort and 0.525, 80.0%, 25.0%, 71.4%, and 28.6% in the testing cohort, respectively (Table 4). By assessing preoperative CT, the AUC, sensitivity, specificity, positive predictive value, and negative predictive value were 0.542, 46.3%, 62.2%, 68.5%, and 39.4% in the training cohort and 0.533, 48.0%, 62.5%, 80.0%, and 27.8% in the testing cohort, respectively (Table 5). The *P* value for statistically comparisons between the AUC of radiomics model and radiologists using baseline CT imaging were < 0.001 and 0.017 respectively in the training and testing cohorts.

Discussion

Our study was a collaborative effort between two centers, with the aim of predicting the presence or absence of LNM in LAGC following NAC. Our radiomics model demonstrated great predictability and reproducibility across centers. Restaging gastric cancer using CT after NAC was thought to be incorrect and unreliable [27]. Our radiomics model, in contrast, outperformed the distinguish between N0 vs. N+ stages on a large scale. Our results showed that the model was more effective in diagnosing patients with or without lymph node metastasis than traditional CT imaging. For example, one enlarged lymph node was diagnosed as metastasis by radiologist at baseline CT, and this node

Table 3 Statistical values of the prediction lymph node metastasis by radiomics score

Radiomics model	Pathological N+	Pathological N0	Area under the curve	Sensitivity	Specificity	Positive predictive value	Negative predictive value
Training cohort			0.846 (95%CI, 0.765–0.926)	81.3%	77.8%	86.7%	70.0%
Radiomic N+	65	10					
Radiomic N0	15	35					
Testing cohort			0.843 (95%CI, 0.701–0.984)	84.0%	75.0%	91.3%	60.0%
Radiomics N+	21	2					
Radiomics N0	4	6					

P value for statistically comparisons: AUC, 0.998; sen, > 0.999; spe, > 0.999; positive predictive value, 0.726; negative predictive value, 0.255
CI confidential interval

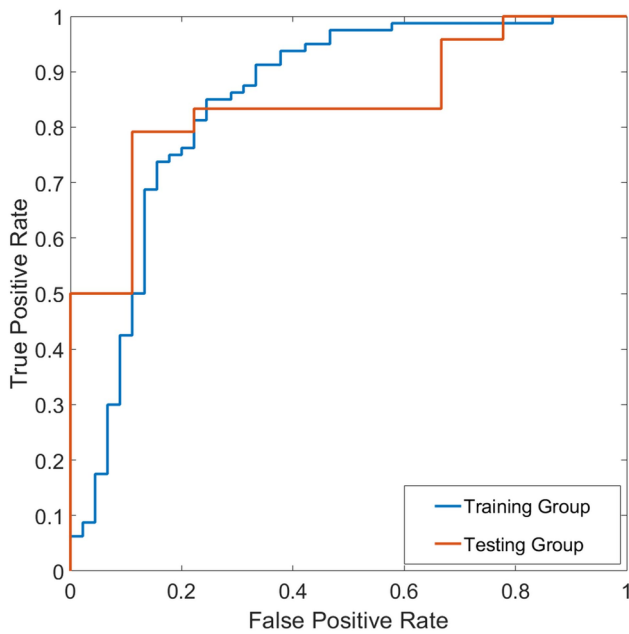


Fig. 2 The areas under the ROC curve of the radiomics model for predicting lymph node metastasis were 0.846 in training group and 0.843 in testing group

shrank after neoadjuvant chemotherapy. It is difficult to determine whether the tumor is still present in this reduced lymph node using CT images (Fig. 3). Conversely, some inflammatory lymph nodes will appear to be enlarged in size, and when the short diameter is greater than 8 mm and with high enhancement, it will be diagnosed as metastasis by the radiologists (Fig. 4). Our radiomics model has significantly higher specificity compared with traditional CT imaging diagnosis and can correct some overstaging of lymph node cases. In recent years, the application of immunotherapy in gastric cancer has been more and more accepted all over the world. The combination immunotherapy performed a higher pathological complete response (pCR) rate than that of chemotherapy alone. A phase II single-arm study of SOX chemotherapy plus anti-PD-1 immunotherapy regimen for locally advanced gastric cancer showed that the postoperative pCR rate reached 26.9% [28]. Our radiomics model has the potential to be applied to the diagnosis of pathological complete response in the future.

Compared to previous investigations on the use of imaging model to predict lymph node metastasis in gastric cancer [20, 22], this study was carried out on tumor ROIs from

Table 4 Statistical values of the prediction lymph node metastasis by baseline CT

CT morphological findings	Pathological N+	Pathological N0	Area under the curve	Sensitivity	Specificity	Positive predictive value	Negative predictive value
Training cohort			0.561 (95%CI, 0.470–0.650)	70.0%	42.2%	68.3%	44.2%
N+ by radiologist	56	26					
N0 by radiologist	24	19					
Testing cohort			0.525 (95%CI, 0.345–0.701)	80.0%	25.0%	76.9%	28.6%
N+ by radiologist	20	6					
N0 by radiologist	5	2					

P value for statistically comparisons: AUC, 0.635; sen, 0.329; spe, 0.455; positive predictive value, 0.167; negative predictive value, 0.684

Table 5 Statistical values of the prediction lymph node metastasis by preoperative CT

CT morphological findings	Pathologic N+	Pathologic N0	Area under the curve	Sensitivity	Specificity	Positive predictive value	Negative predictive value
Training cohort			0.542 (95%CI, 0.451–0.632)	46.3%	62.2%	68.5%	39.4%
N+ by radiologist	37	17					
N0 by radiologist	43	28					
Testing cohort			0.533 (95%CI, 0.351–0.708)	48.0%	62.5%	80.0%	27.8%
N+ by radiologist	12	3					
N0 by radiologist	13	5					

P value for statistically comparisons: AUC, 0.942; sen, > 0.999; spe, > 0.999; positive predictive value, 0.526; negative predictive value, 0.360

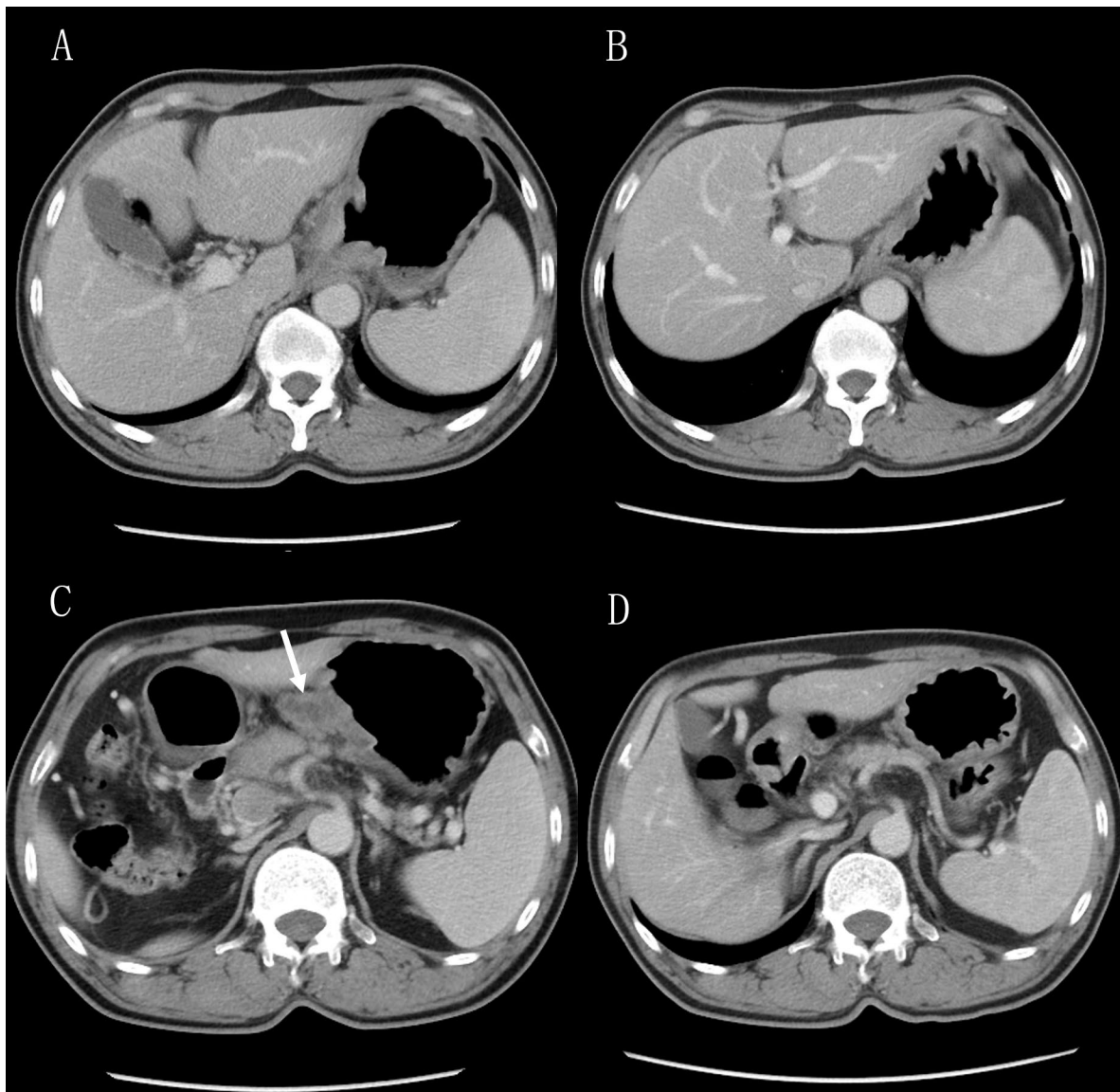


Fig. 3 A–D A 59-year-old male patient with gastric adenocarcinoma. He received radical gastrectomy after 3 cycles of neoadjuvant chemotherapy. Pathological results showed that there was no tumor cell residue in the stomach. Some changes after chemotherapy, including lymphocyte and foam cell infiltration and interstitial fibrosis, were observed in the gastric surgical specimen. No lymph node metastasis was detected. The pathological stage was ypT0N0 stage. **A** An ulcerative tumor of the gastric cardia was found on axial CT with sig-

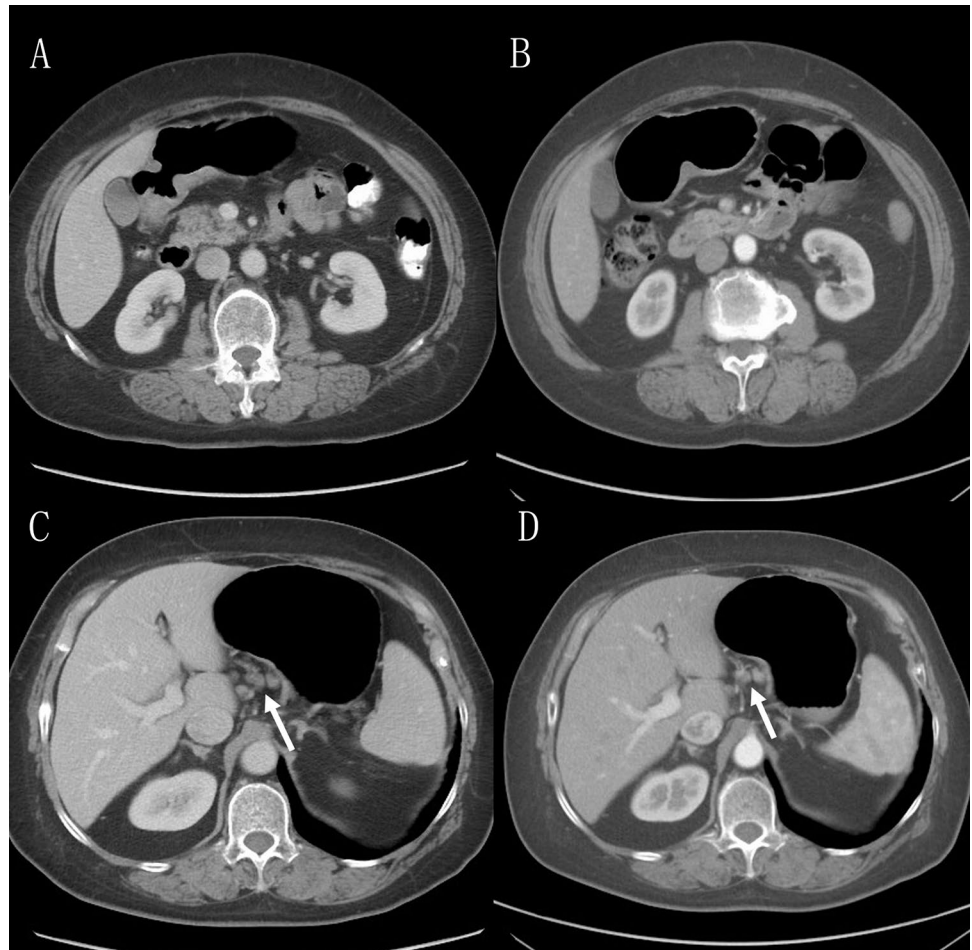
nificant enhancement in baseline examination. **B** After neoadjuvant chemotherapy, the thickness of gastric wall in the cardia was reduced. **C** A 36*25 mm enlarged lymph node (arrow) with central necrosis was detected at the lesser curvature area of stomach. This node was diagnosed as metastatic by the radiologist. **D** This lymph node was significantly reduced after chemotherapy with the size of 7*5 mm. The radiomics model and radiologist both wrongly diagnosed the patient as lymph node metastasis (N+ stage) after chemotherapy

multiphase CT images of baseline and pre-operative CT scans rather than on one ROI from a single CT phase. In addition, we added image ROI data of two enlarged lymph nodes to the model. The imaging information of lymph node itself plays a complementary role in the diagnosis of N0. In medical terms, this makes radiomics models predicting lymph node metastasis more explicable. Using radiology features to predict pathological complete response after NAC is a potential component of treatment strategy for

patients with LAGC. Those patients who had a pathological complete response after NAC would get significantly better survival outcomes [8].

In this study, 2D features were extracted from the ROI delineated on the largest slice. Compared with 3D features, 2D features are insensitive to the anisotropic scanning. In both training and testing groups, the intra-slice resolution is around 0.7 mm×0.7 mm, but the inter-slice resolution is around 5.0 mm. If 3D features are used, isotropic

Fig. 4 A–D A 62-year-old female patient with adenocarcinoma of antrum of stomach. Postoperative pathological stage was ypT3N0 stage. No lymph node metastasis was detected in pathological results. **A** The thickened gastric wall in the antrum was found on axial CT in baseline examination. **B** After neoadjuvant chemotherapy, gastric wall thickening, and enhancement decreased. **C** Three enlarged lymph nodes with cluster distribution (arrow) were detected at the lesser curvature area of stomach. The largest lymph nodes are 13*10 mm in size. Radiologist diagnosed the patient with lymph node metastasis. **D** These lymph nodes shrank slightly after chemotherapy, with the largest node shrinking to 10*8 mm. According to the diagnostic criteria of CT imaging, these three lymph nodes were diagnosed as metastases by the radiologist after chemotherapy. However, the pathological stage was N0 stage. The radiomics model correctly diagnosed the patient as stage N0



resampling is required. However, the influence from resampling still needs investigation. In contrary, 2D features are more robust, and resampling is not needed. The authors selected 13 features in the linear model, and the 2 features with largest weight are post-treatment Zone% feature in venous phase and post-treatment low gray level zone emphasis in venous phase. Both of these two features are related with the percentage of subregions in tumor ROI, especially with the percentage of low-signal subregions. Although the weight of other features are relatively less, they also reflects the changes in the tumor and lymph nodes before and after chemotherapy from the perspective of the image texture features. But in current studies, it is difficult to explain the relationship between each feature and clinical significance from a medical perspective. The negative weights show that both features are negatively related with the probability of LN metastasis. Probably, the high percentage of low-signal subregions is caused by an increase of necrosis or fibrosis after NAC, which is an indicator of good response to NAC.

Our study had some limitations. First, this is a retrospective research, which might be with selection bias and

small sample size, though it is a two-center analysis. Second, we built the model using single-layer images of the maximum length diameter of the tumor and lymph nodes, which may not represent all informations about the tumor due to the heterogeneity within the tumor. In future studies, further modeling studies with tumor and lymph node volume image should be considered. Due to the large workload of repeatedly delineating the ROI of gastric cancer, intrareader/interreader reproducibility of radiomics features were not performed in this study.

In conclusion, we demonstrated that radiomics models using baseline and restaging CT offered good predictive value for the presence of lymph node metastasis after NAC. The model had the potential to be applied to the prediction of pathological complete response in the future.

Author Contribution Q.Y. and Y.S. contributed to the conception and design of the study. All authors participated in the clinical practice, including diagnosis, treatment, consultation, and follow-up of patients. Z.W. and H.Z. contributed to the acquisition of data. Q.Y. and J.S. contributed to the analysis of data. J.S. wrote the manuscript. Q.Y. and Z.W. revised the manuscript. All authors approved the final version of the manuscript.

Funding This work was supported by the Beijing Municipal Administration of Hospitals Incubating Program (PX2024039), the Beijing Hospitals Authority' Ascent Plan (DFL20191103), and the Beijing Hospitals Authority Youth Programme (QML 20190308).

Data Availability The datasets generated and analyzed during the current study are available from the corresponding author on reasonable request.

Declarations

Ethics Approval and Consent to Participate This retrospective study was authorized and approved by the Ethics Committee of Peking University Cancer Hospital (approval number: 2019KT105), and informed consent was waived due to retrospective nature.

Consent for Publication Not applicable.

References

- Health Commission Of The People's Republic Of China N (2009) National guidelines for diagnosis and treatment of gastric cancer 2022 in China (English version). *Chin J Cancer Res* 30(34):207–237. <https://doi.org/10.21147/j.issn.1000-9604.2022.03.04>.
- Sitarz R, Skierucha M, Mielko J, Offerhaus GJA, Maciejewski R, Polkowski WP (2018) Gastric cancer: epidemiology, prevention, classification, and treatment. *Cancer Manag Res* 10:239–248. <https://doi.org/10.2147/CMAR.S149619>.
- Bray F, Ferlay J, Soerjomataram I, Siegel RL, Torre LA, Jemal A (2018) Global cancer statistics 2018: GLOBOCAN estimates of incidence and mortality worldwide for 36 cancers in 185 countries. *CA Cancer J Clin* 68:394–424. <https://doi.org/10.3322/caac.21492>
- Ajani JA, D'Amico TA, Bentrem DJ, Chao J, Cooke D, Corvera C, et al (2022) Gastric Cancer, Version 2.2022, NCCN Clinical Practice Guidelines in Oncology. *J Natl Compr Canc Netw* 20:167–192. <https://doi.org/10.6004/jnccn.2022.0008>.
- Ao S, Wang Y, Song Q, Ye Y, Lyu G (2021) Current status and future perspectives on neoadjuvant therapy in gastric cancer. *Chin J Cancer Res* 33:181–192. <https://doi.org/10.21147/j.issn.1000-9604.2021.02.06>.
- Kwee RM, Kwee TC (2009) Imaging in assessing lymph node status in gastric cancer. *Gastric Cancer* 12:6–22. <https://doi.org/10.1007/s10120-008-0492-5>.
- Wang ZL, Li YL, Li XT, Tang L, Li ZY, Sun YS (2021) Role of CT in the prediction of pathological complete response in gastric cancer after neoadjuvant chemotherapy. *Abdom Radiol (NY)* 46:3011–3018. <https://doi.org/10.1007/s00261-021-02967-3>.
- Li Z, Shan F, Wang Y, Zhang Y, Zhang L, Li S, et al (2018) Correlation of pathological complete response with survival after neoadjuvant chemotherapy in gastric or gastroesophageal junction cancer treated with radical surgery: A meta-analysis. *PLoS One* 13:e0189294. <https://doi.org/10.1371/journal.pone.0189294>.
- Kwee RM, Kwee TC (2014) Role of imaging in predicting response to neoadjuvant chemotherapy in gastric cancer. *World J Gastroenterol* 20:1650–6. <https://doi.org/10.3748/wjg.v20.i7.1650>.
- Lee JJ, Lee JM, Kim SH, Shin CI, Lee JY, Kim SH, et al (2010) Diagnostic performance of 64-channel multidetector CT in the evaluation of gastric cancer: differentiation of mucosal cancer (T1a) from submucosal involvement (T1b and T2). *Radiology* 255:805–14. <https://doi.org/10.1148/radiol.10091313>.
- Giganti F, Tang L, Baba H (2019) Gastric cancer and imaging biomarkers: Part 1 - a critical review of DW-MRI and CE-MDCT findings. *Eur Radiol* 29:1743–1753. <https://doi.org/10.1007/s00330-018-5732-4>.
- Chen CY, Hsu JS, Wu DC, Kang WY, Hsieh JS, Jaw TS, et al (2007) Gastric cancer: preoperative local staging with 3D multi-detector row CT—correlation with surgical and histopathologic results. *Radiology*. 2007;242:472–82. <https://doi.org/10.1148/radiol.2422051557>.
- Fukuya T, Honda H, Hayashi T, Kaneko K, Tateshi Y, Ro T, et al (1995) Lymph-node metastases: efficacy for detection with helical CT in patients with gastric cancer. *Radiology* 197:705–11. <https://doi.org/10.1148/radiology.197.3.7480743>.
- D'Elia F, Zingarelli A, Palli D, Grani M (2000). Hydro-dynamic CT preoperative staging of gastric cancer: correlation with pathological findings. A prospective study of 107 cases. *Eur Radiol* 10(12):1877–85. <https://doi.org/10.1007/s003300000537>.
- Habermann CR, Weiss F, Riecken R, Honarpisheh H, Bohnacker S, Staedtler C, et al (2004). Preoperative staging of gastric adenocarcinoma: comparison of helical CT and endoscopic US. *Radiology* 230(2):465–71. <https://doi.org/10.1148/radiol.2302020828>.
- Kim AY, Kim HJ, Ha HK (2005). Gastric cancer by multidetector row CT: preoperative staging. *Abdom Imaging* 30(4):465–72. <https://doi.org/10.1007/s00261-004-0273-5>.
- Kim HS, Han HY, Choi JA, Park CM, Cha IH, Chung KB, et al (2001). Preoperative evaluation of gastric cancer: value of spiral CT during gastric arteriography (CTGA). *Abdom Imaging* 26(2):123–30. <https://doi.org/10.1007/s002610000167>.
- Kim HJ, Kim AY, Oh ST, Kim JS, Kim KW, Kim PN, et al (2005). Gastric cancer staging at multi-detector row CT gastrography: comparison of transverse and volumetric CT scanning. *Radiology* 236(3):879–85. <https://doi.org/10.1148/radiol.2363041101>.
- Chen J, Cheong JH, Yun MJ, Kim J, Lim JS, Hyung WJ, et al (2005) Improvement in preoperative staging of gastric adenocarcinoma with positron emission tomography. *Cancer* 103(11):2383–90. <https://doi.org/10.1002/cncr.21074>.
- Park SR, Lee JS, Kim CG, Kim HK, Kook MC, Kim YW, Ryu KW, Lee JH, Bae JM, Choi IJ (2008) Endoscopic ultrasound and computed tomography in restaging and predicting prognosis after neoadjuvant chemotherapy in patients with locally advanced gastric cancer. *Cancer* 112:2368–76. <https://doi.org/10.1002/cncr.23483>.
- Lambin P, Leijenaar RTH, Deist TM, Peerlings J, de Jong EEC, van Timmeren J, et al (2017) Radiomics: the bridge between medical imaging and personalized medicine. *Nat Rev Clin Oncol*. 2017;14:749–762. <https://doi.org/10.1038/nrclinonc.2017.141>
- Dong D, Fang MJ, Tang L, Shan XH, Gao JB, Giganti F, et al (2020) Deep learning radiomic nomogram can predict the number of lymph node metastasis in locally advanced gastric cancer: an international multicenter study. *Ann Oncol*. 2020;31:912–920. <https://doi.org/10.1016/j.annonc.2020.04.003>.
- Dong D, Tang L, Li ZY, Fang MJ, Gao JB, Shan XH, et al (2019) Development and validation of an individualized nomogram to identify occult peritoneal metastasis in patients with advanced gastric cancer. *Ann Oncol*. 2019;30:431–438. <https://doi.org/10.1093/annonc/mdz001>.
- Yang J, Wu Q, Xu L, Wang Z, Su K, Liu R, et al (2020) Integrating tumor and nodal radiomics to predict lymph node metastasis in gastric cancer. *Radiother Oncol*. 2020;150:89–96. <https://doi.org/10.1016/j.radonc.2020.06.004>.
- Jiang Y, Zhang Z, Yuan Q, Wang W, Wang H, Li T, et al (2022) Predicting peritoneal recurrence and disease-free survival from CT images in gastric cancer with multitask deep learning: a retrospective study. *Lancet Digit Health* 4:e340–e350. [https://doi.org/10.1016/S2589-7500\(22\)00040-1](https://doi.org/10.1016/S2589-7500(22)00040-1).
- E A Eisenhauer, P Therasse, J Bogaerts, et al. New response evaluation criteria in solid tumours: revised RECIST guideline (version 1.1). *Eur J Cancer* 2009; 45(2):228–47. <https://doi.org/10.1016/j.ejca.2008.10.026>.

27. Yoshikawa T, Tanabe K, Nishikawa K, Ito Y, Matsui T, Kimura Y, et al (2014) Accuracy of CT staging of locally advanced gastric cancer after neoadjuvant chemotherapy: cohort evaluation within a randomized phase II study. *Ann Surg Oncol* 21 Suppl 3:S385-9. <https://doi.org/10.1245/s10434-014-3615-8>.
28. Xuewei Ding, Xuejun Wang, Bin Li, Longgang Wang, Honghai Guo, Liang Shang, et al (2023) PERSIST: A multicenter, randomized phase II trial of perioperative oxaliplatin and S-1 (SOX) with or without sintilimab in resectable locally advanced gastric/gastroesophageal junction cancer (GC/GEJC). *Journal of Clinical Oncology* 41:4_suppl, 364–364. https://doi.org/10.1200/JCO.2023.41.4_suppl.364

Publisher's Note Springer Nature remains neutral with regard to jurisdictional claims in published maps and institutional affiliations.

Springer Nature or its licensor (e.g. a society or other partner) holds exclusive rights to this article under a publishing agreement with the author(s) or other rightsholder(s); author self-archiving of the accepted manuscript version of this article is solely governed by the terms of such publishing agreement and applicable law.